Flexocoupling-induced soft acoustic modes and the spatially modulated phases in ferroelectrics

Anna N. Morozovska,[1,2,*] Maya D. Glinchuk,[3] Eugene A. Eliseev,[3] and Yulian M. Vysochanskii[4,†]
[1]*Institute of Physics, National Academy of Sciences of Ukraine, 46, Prospekt Nauky, 03028 Kyiv, Ukraine*
[2]*Bogolyubov Institute for Theoretical Physics, National Academy of Sciences of Ukraine, 14-b Metrolohichna Street 03680 Kyiv, Ukraine*
[3]*Institute for Problems of Materials Science, National Academy of Sciences of Ukraine, 3, Krjijanovskogo, 03142 Kyiv, Ukraine*
[4]*Institute of Solid State Physics and Chemistry, Uzhgorod University, 88000 Uzhgorod, Ukraine*
(Received 17 May 2017; revised manuscript received 15 August 2017; published 29 September 2017)

Using the Landau-Ginzburg-Devonshire theory and one component approximation, we examined the conditions of the soft acoustic phonon mode (**A**-mode) appearance in a ferroelectric (FE) depending on the magnitude of the flexoelectric coefficient f and temperature T. If the flexocoefficient f is equal to the temperature-dependent critical value $f^{cr}(T)$ at some temperature $T = T_{IC}$, the **A**-mode frequency tends to zero at wave vector $k = k_0^{cr}$, and the spontaneous polarization becomes spatially modulated in the temperature range $T < T_{IC}$, where T_{IC} is turned into the transition temperature to the incommensurate spatially modulated phase (SMP). When $f > f^{cr}(T_{IC})$, the **A**-mode becomes zero for two wave vectors $k = k_{1,2}^{cr}$, and does not exist in the range of wave vectors $k_1^{cr} < k < k_2^{cr}$, indicating the transition to SMP. The corresponding temperature dependence of the dielectric susceptibility is in agreement with experimental data in ferroics with SMPs. This gives us a background to predict flexocoupling-induced soft acoustic amplitudon-type modes in FEs with SMPs of type II. The available experimental results on neutron scattering in organic incommensurate FE betaine calcium chloride dihydrate are in semiquantitative agreement with our theoretical results.

DOI: 10.1103/PhysRevB.96.094111

I. INTRODUCTION

Dynamical characteristics of phase transitions in ferroics have attracted great attention from scientists for many years, being the source of valuable information for fundamental physical research and advanced applications [1,2]. Typically, the phase transitions lead to the instability of soft phonon modes [3]. In particular, for ferroelectrics (FEs), the frequency ω_{TO} of transverse optic (TO) soft phonon mode depends on temperature T so that $\omega_{TO}(T_C) = 0$ at transition temperature $T = T_C$.

Basic experimental methods, which contain information about soft phonon modes and spatial modulation of the order parameter in ferroics (such as anti-FEs, proper, and incipient FEs), are dielectric measurements [4], inelastic neutron scattering [3,5–10], x-ray [11–14], Raman [15], and Brillouin [11,14,16–19] scatterings, and the ultrasonic pulse-echo method [16,18], allowing hypersound spectroscopic measurements.

Scattering experiments proved that, not only does the TO mode soften substantially with decreasing temperature to freeze out at T_C in ferroics (such as FE perovskites), but also finite wave vector anomalies appear in the transverse acoustic (TA) mode for structural phase transitions [20–22]. In particular, Cowley [20] measured the softening of the TA mode in $SrTiO_3$ at (105–110) K. The acoustic soft mode was observed in the incipient FE $SrTiO_3$ near the structural antiferrodistortive phase transition by Bussmann-Holder *et al.* [23], and the authors supposed that such behavior is driven by polar optic soft mode. Axe *et al.* [5] experimentally studied the coupling between TA and TO modes in $KTaO_3$ at different temperatures. The pronounced softening of the TA mode has been revealed in betaine calcium chloride dihydrate $[(CH_3)_3NCH_2COO{\cdot}CaCl_2{\cdot}2H_2O]$ by Hlinka *et al.* [9]. The linear interaction of acoustic mode and soft optic mode leads to pronounced softening of the TA mode manifesting itself in the remarkable lowering of hypersound velocity for the TA phonons observed in the incommensurate FE $Sn_2P_2(Se_xS_{1-x})_6$ in the vicinity of the Lifshitz point (LP) [16]. The flexoelectric coupling-induced interaction of TA and TO modes in anti-FE $PbZiO_3$ led to the recent paper by Tagantsev *et al.* [12]. Besides these original papers, lots of information about experimental and theoretical investigations of soft modes in different ferroics can be found in the seminal textbooks [1,24,25].

However, the question about the type of soft modes, which cannot be optic ones in the incommensurate spatially modulated phases (SMPs) of ferroics, is still highly relevant, although mechanisms and details of the incommensurate SMPs' appearance in solids have become the subject of many theoretical and experimental studies since early 1970s [1,5,20] until nowadays [9,12,16]. In particular, the transition to the incommensurate phase is a question that has not been explored in detail yet, while the very idea of Axe *et al.* [5] is that the TO-TA mode coupling causes the instability of the TA mode at some temperature that, in turn, leads to the appearance of an incommensurate phase. Notably, the idea based on the static flexoelectric coupling between polarization and strain gradients (in the form of a tensorial Lifshitz invariant) was used by Tagantsev *et al.* (see Eq. (4) in Ref. [12]) to explain the origin of antiferroelectricity in $PbZiO_3$. To estimate the TO-TA mode coupling and incommensurate SMP appearance in proper FEs, Kohutych *et al.* [16] included the flexoelectric term in the form of Lifshitz invariant $\frac{f}{2}(P\frac{\partial u}{\partial x} - u\frac{\partial P}{\partial x})$, where P is polarization component, u is the strain component, and f is the static flexoelectric coefficient.

Having mentioned the impact of the Lifshitz invariant $\frac{f}{2}(\xi\frac{\partial \eta}{\partial x} - \eta\frac{\partial \xi}{\partial x})$ relating the order parameters ξ and η on the appearance of the incommensurate phase, it is necessary to discuss the adopted classification of incommensurate phases

*anna.n.morozovska@gmail.com
†vysochanskii@gmail.com

in ferroics. Following Bruce *et al.* [26], the consideration of incommensurate phases based on the Landau theory of phase transitions, it is customary to distinguish two cases, those in which the symmetry of the order parameter(s) is such that the Lifshitz invariant can exist (called incommensurate phases of type I) and those in which the invariant is absent (called incommensurate phases of type II). From the beginning most of the Landau theory-based theoretical studies considered type I phases (see, e.g., Golovko [27] and Levanyuk *et al.* [28]), the studies of the type II phases were more rare (see, e.g., Hornreich *et al.* [29] and Golovko [30]).

Since the direct and converse static flexoelectric effects, which lead to the appearance of polarization due to the strain gradient and vice versa [31,32], exist in a ferroic of arbitrary symmetry [33–35], the tensorial Lifshitz invariant $\frac{f_{klij}}{2}(P_i \frac{\partial u_{kl}}{\partial x_j} - u_{kl} \frac{\partial P_i}{\partial x_j})$ should be included to the free energy functional of all those ferroics for which the polarization component(s) P_i is a primary order parameter. Also, the invariant can be included if the polarization is a secondary order parameter, but in this case, P_i should be expressed via the primary order parameter(s). It was shown that the flexocoupling term in the form of a Lifshitz invariant can induce incommensurate SMPs in many ferroics, including anti-FE and antiferrodistortive ones [12,36–38].

Note that the static flexoelectric effect is omnipresent from the symmetry theory considerations (in the sense that f_{klij} has nonzero components for any point symmetry), and the earliest [32] and recent [39,40] microscopic calculations give nonzero (and sometimes rather high) values of flexoelectric coefficients for many FEs. It is possible to define the static flexoelectric coefficients from direct experiments [41–43], as well as from the fitting of soft phonon spectra in FEs (see, e.g., Ref. [44] and refs. therein).

From considerations of the symmetry theory stating that all terms and invariants, whose existence does not violate the symmetry of the system, are allowed, Tagantsev *et al.* [12] predicted the existence of a cross-term in the kinetic energy $M_{ij} \frac{\partial P_i}{\partial t} \frac{\partial U_j}{\partial t}$ and named it dynamic flexoelectric effect, as it originates from the cross-term of polarization and elastic displacement time derivatives $\frac{\partial P_i}{\partial t} \frac{\partial U_j}{\partial t}$ (see reviews [45,46] and references therein). At present, the situation with the magnitudes M_{ij} of dynamic flexoeffect is more complex and controversial than for the static one because there are microscopic theories in which the effect is absent. Namely, Stengel [47] has shown that, since both polarization and elastic displacement are supposed to be normal modes of the crystal at the center of Brillouin zone, they should diagonalize the dynamical matrix, leading to the absence of the cross-term in the matrix. It should be noted that the Stengel result [47] was argued later on by Kvasov and Tagantsev [48], who evaluated the strength of the dynamic flexoelectric effect in $SrTiO_3$ from microscopic calculations, and it appeared comparable to that of the static bulk flexoelectric effect. More discussion of the problem can be found in Refs. [44,49].

The impact of dynamic flexoelectric coupling on the soft phonon spectra in ferroics has not been studied until recently [48,50,51]. Note that the best fitting of the soft phonon spectra observed in $SrTiO_3$, $PbTiO_3$, $Sn_2P_2S_6$, and $Sn_2P_2Se_6$ performed by Morozovska *et al.* [50,51] corresponds to nonzero values of dynamic flexoelectric coefficient, which are of the same order as the ones calculated by Kvasov and Tagantsev [48]. However, the indirect evidences followed from the fitting with many parameters [50,51] cannot be the crucial argument, and so we believe that direct measurements of the static and dynamic flexoelectric coefficients are urgently required.

Since a wave excitation of any nature is impossible without a local gradient of the corresponding physical quantity [52,53], the static and dynamic flexoelectric effects should influence the propagation of acoustic waves in all solids, although the effect should be more pronounced for short than for long wavelengths [54]. For example, an acoustic wave will be inevitably accompanied by a local gradient of mechanical strains and stresses. Due to the direct static flexoelectric effect, the wave of the strain gradient induces the wave of the electric polarization, even in the paraelectric (PE) phase (i.e., local polarization, the mean value of which is zero). The local polarization gradient, due to the converse flexoelectric effect, will affect the elastic stresses associated with the wave.

Recently, to extend the Axe *et al.* theory [5], Morozovska *et al.* [50,51] used the Landau-Ginzburg-Devonshire (LGD) approach to consider the influence of the flexocoupling on the appearance of SMPs, and on the properties of optic and acoustic phonons in the FE and PE phases of FEs $PbTiO_3$, $Sn_2P_2(S,Se)_6$, and PE $SrTiO_3$. In order to derive the analytical expressions from the LGD free energy, which includes the higher gradient terms, static flexocoupling in the form of a Lifshitz invariant and dynamical flexoelectric effect in the form proposed by Kvasov and Tagantsev [48], we were subjected to restriction of our consideration by one component of the polarization and strain. These restrictions can be called the one component approximation [51]. The consequence of this approximation is the occurrence of only one optical and one acoustic mode, which interact via electrostriction and flexoelectric couplings.

Allowing we are interested in SMP transition that does not belong to the FE one [55], optic modes are not suitable to be soft ones at the transition. In the following sections, we are going to consider mainly acoustic mode dispersion and its temperature dependence.

The simplified dispersion law cannot describe the interaction between different transverse and longitudinal optical modes and three acoustic modes induced by cooperative effects, flexoelectric, and electrostriction couplings in the FE phase of multiaxial FEs. Moreover, the coupling between different optic phonon modes can either act cooperatively with the flexocoupling or against it [see, e.g., the models by Kappler and Walker [56] and Hlinka *et al.* [57] adopted for organic FEs such as $(CH_3)_3NCH_2COO{\cdot}CaCl_2{\cdot}2H_2O$]. If acoustic and optic modes are considered, their mutual coupling contributes to the SMP appearance, similarly to the flexoelectricity standing alone [57]. Actually, it was shown that elastic softening in the hypersound range in $Sn_2P_2(Se_xS_{1-x})_6$ is induced mostly by linear interaction between soft optic and acoustic phonon branches, so that the Landau-Khalatnikov model explains temperature dependence of hypersound velocity in the FE phase [16].

Taking into account the limitations of the one component approximation validity, we can reasonably apply the analytical

results to describe the experimentally observed phonon dispersion in uniaxial ferroics only, e.g., for the monoclinic FEs $Sn_2P_2(Se_xS_{1-x})_6$ [58,59], as well as in the PE phase of organic FEs, like $(CH_3)_3NCH_2COO{\cdot}CaCl_2{\cdot}2H_2O$ [9], if the interaction between different phonon modes appeared relatively small at high temperatures.

Motivated by the above argumentation, we derived analytical expressions for the singular points (zero points, complex ranges) of the **A**-mode frequency $\omega(k)$ dependent on the wave vector k and examined the conditions of the soft acoustic mode appearance in FEs depending on the magnitude of the flexoelectric coefficient and temperature in this paper.

II. ANALYTICAL ONE COMPONENT THEORY

Using LGD theory and one component approximation in the considered one-dimensional (1D) case, the Lagrange function $L = \int_t dt \int_{-\infty}^{\infty} dx(F - K)$ consists of the kinetic energy K and free energy F of a FE [45,46]. Following Ref. [51], the density of kinetic energy

$$K = \frac{\mu}{2}\left(\frac{\partial P}{\partial t}\right)^2 + M\frac{\partial P}{\partial t}\frac{\partial U}{\partial t} + \frac{\rho}{2}\left(\frac{\partial U}{\partial t}\right)^2, \qquad (1)$$

includes the dynamic flexocoupling [45,46,48] with the magnitude M; ρ is the density of a material; μ is a kinetic coefficient. The elastic displacement component U is related to the strain u as $u = \partial U/\partial x$.

The bulk density of the free energy F that depends on polarization component P and strain component u, and their gradients, has the following form [51]:

$$F = \frac{\alpha}{2}P^2 + \frac{\beta}{4}P^4 + \frac{\gamma}{4}P^6 + \frac{g}{2}\left(\frac{\partial P}{\partial x}\right)^2 - quP^2 - \frac{f}{2}\left(P\frac{\partial u}{\partial x} - u\frac{\partial P}{\partial x}\right) + \frac{c}{2}u^2 + \frac{v}{2}\left(\frac{\partial u}{\partial x}\right)^2 - PE - NU. \qquad (2)$$

According to the Landau theory [60,61], the coefficient α linearly depends on the temperature T for proper FEs $\alpha(T) = \alpha_T(T - T_C)$. Here, T_C is the Curie temperature. All other coefficients in Eq. (2) are supposed to be temperature independent. The coefficient $\beta > 0$ for the FEs with the second-order phase transition, and $\beta < 0$ for the first-order one. The coefficient $\gamma \geqslant 0$ for the stability of the free energy for all P values. The gradient coefficients g and v determine the magnitude of the gradient energy. The coefficient f is the component of the static flexocoupling tensor. The elastic stiffness c should be positive for the functional stability. The electrostriction coefficient q can be positive or negative. The polarization interacts with an external electric field E. Also, N is the bulk density of external mechanical force.

We did not include the term $PE_d/2$ in Eq. (2), assuming that the depolarization field E_d is absent. The case corresponds to the transverse fluctuations of polarization, which we consider and regard that the longitudinal fluctuations of polarization are much smaller due to the depolarization field [55].

Unlike our previous work [51], we did not included the higher polarization gradient term proportional to $w(\partial^2 P/\partial x^2)^2$ in Eq. (1) and therefore consider only positive $g > 0$. This is done in order to study those and only those types of SMPs which are driven by the flexocoupling only, due the presence of the Lifshitz invariant $\frac{f}{2}(P\frac{\partial u}{\partial x} - u\frac{\partial P}{\partial x})$ in Eq. (1). The higher polarization gradient term determines the possible appearance of the minima on the optic mode frequency and so promotes the appearance of an incommensurate phase with increase of its strength w (see, e.g., Figs. 1 and 2 in review [62]). We regard that it is really important to distinguish between the scenario of SMP origin in initially homogeneous commensurate ferroics (with $g > 0$ and $w = 0$) under the flexocoupling strength f increase [37] from other possible scenarios of incommensurate SMP appearance in different ferroics (see Ref. [62] and refs. therein).

The strain gradient coefficient v is typically omitted in the free energy of ferroics, despite that its necessity under the presence of flexocoupling had been established [40,63–65]. If the expansion in Eq. (1) is cut on the strain-gradient squared term (as in our case), the necessary condition of the free energy global minimum (as opposed to the maximum or saddle point) requires the positive sign of the coefficient v. If v is negative, it is necessary to take into account the further terms of the expansion (together with higher derivatives of polarization) in order to obtain a self-consistent theory. Unfortunately, we did not know the direct way of v determination from experiments that is fully reliable and unambiguous, and so its calculations from the first principles are in order. Following the first principle calculations of Maranganti and Sharma [66], the conclusion $v < 0$ steams from the dispersion of the acoustic branch, whose frequency dependence on the wave vector usually curves downward. However, the conclusion [66] is valid in the framework of the "oversimplified" theory, without any coupling with other modes. Approach [50,51] shows that the "down" or "up" bending of the dispersion curve is determined at least by three parameters, v, M, and f, and the latter is responsible for the coupling (attraction or repulsion) between acoustic and optic modes. Comparison of the phonon spectra observed in different perovskites with the phenomenological theory performed in Ref. [51] shows that the best fitting of the observed spectra is possible for positive values of v when taking into account the lattice discreteness (see e.g. Fig. 4 and Table I in Ref. [51]). However, the fitting procedure used in Refs. [50,51] is indirect and so its results cannot solve the controversy with atomic simulations leading to the negative values of v for some materials. Perhaps there is no contradiction because, according to Stengel [40], the lattice discreteness is one of the possibilities to avoid considering negative strain-gradient squared energy.

Using the methodology described in detail in Refs. [50,51], the dynamic equations of state are obtained from the variation of the Lagrange function L on P and U. The dependence of the soft phonon frequency $\omega(k)$ on its wave vector k can be calculated from the linearized time-dependent dynamic equations of state for the polarization and elastic displacement components P and U, correspondingly (see Appendix A in the Supplemental Material [67]). After the linearization of the equations, the solution acquires the form of the Fourier integrals $P = P_S + \int dtdke^{ikx-i\omega t}\tilde{P}(\omega,k)$, $u = u_S + \int dtdke^{ikx-i\omega t}\tilde{u}(\omega,k)$, $E = \int dtdke^{ikx-i\omega t}\tilde{E}(\omega,k)$, and $N = \int dtdke^{ikx-i\omega t}\tilde{N}(\omega,k)$, where the spontaneous

values $P_S^2 = (\sqrt{\beta^{*2} - 4\alpha\gamma} - \beta^*)/2\gamma$ and $u_S = qP_S^2/c$ are nonzero in the long-range ordered phases; and coefficient $\beta^* = (\beta - 2q^2/c)$. As a result, the polarization $\tilde{P}$ and elastic displacement $\tilde{U}$ are linearly proportional to external electric field and mechanical force variations $\tilde{E}$ and $\tilde{N}$. The solution has the matrix form

$$\begin{pmatrix} \tilde{P} \\ \tilde{U} \end{pmatrix} = \begin{bmatrix} \tilde{\chi}(k,\omega) & \tilde{\eta}(k,\omega) \\ \tilde{\eta}^*(k,\omega) & \tilde{\vartheta}(k,\omega) \end{bmatrix} \begin{pmatrix} \tilde{E} \\ \tilde{N} \end{pmatrix}, \tag{3a}$$

where the matrix elements (generalized susceptibilities) are given by expressions:

$$\tilde{\chi}(k,\omega) = \frac{vk^4 + ck^2 - \rho\omega^2}{\Delta(k,\omega)},$$

$$\tilde{\eta}(k,\omega) = -\frac{fk^2 - M\omega^2 - 2iqkP_S}{\Delta(k,\omega)}, \tag{3b}$$

$$\tilde{\vartheta}(k,\omega) = \frac{\alpha_S + gk^2 - \mu\omega^2}{\Delta(k,\omega)},$$

$$\Delta(k,\omega) = (\alpha_S + gk^2 - \mu\omega^2)(vk^4 + ck^2 - \rho\omega^2) - (fk^2 - M\omega^2)^2 + 4k^2q^2P_S^2. \tag{3c}$$

Hereinafter, the positive temperature-dependent function $\alpha_S(T)$ is introduced

$$\alpha_S(T) = \alpha(T) + \left(3\beta - 2\frac{q^2}{c}\right)P_S^2(T) + 5\gamma P_S^4(T). \tag{4}$$

Below, we will be interested in the linear dielectric susceptibility $\tilde{\chi}(k,\omega)$, since $\tilde{N} = 0$ in the considered case.

Using the results of Ref. [51], the condition $\Delta(k,\omega) = 0$ gives us the biquadratic equation for the frequency $\omega(k)$, $(\mu\rho - M^2)\omega^4 - C(k)\omega^2 + B(k) = 0$. The solution of the biquadratic equation can be represented in the form

$$\omega_{1,2}^2(k) = \frac{C(k) \pm \sqrt{C^2(k) - 4(\mu\rho - M^2)B(k)}}{2(\mu\rho - M^2)}, \tag{5}$$

where the functions $C(k) = \alpha_S\rho + (c\mu - 2fM + g\rho)k^2 + \mu vk^4$ and $B(k) = k^2(\alpha_S c - 4q^2P_S^2 + (cg + \alpha_S v - f^2)k^2 + gvk^4)$, respectively. The dispersion relation in Eq. (5) contains one optical (**O**) phonon mode and one acoustic (**A**) phonon mode, which correspond to the signs "+" and "−" before the radical, respectively. The **O** mode is in fact transverse, and the **A** mode can be longitudinal or transverse. Note that the **A** mode $\omega_2(k)$ is independent on the flexocoupling at very small k, namely $\omega_2(k \to 0) \cong (\sqrt{c/\rho})k$.

Note that the analytical expressions for $\tilde{\chi}(k,\omega)$ and $\omega(k)$ look simpler that the corresponding expressions (21) and (23) in Ref. [51] due to the condition $w = 0$.

III. SOFT ACOUSTIC MODE IN THE SMP

A. The critical points in the soft phonon spectra

The dependence of the **O** mode on the flexocoupling constant is weak and noncritical at small k. The softening law of the optical phonons is valid near Curie temperature T_C, $\omega(T) \sim \sqrt{\alpha_S(T)} \sim \sqrt{|T_C - T|}$. However, the flexocoupling leads to the fact that the condition $\omega^2 = 0$ can be valid for the **A** mode not only at $k = 0$, but also at $k = k_{cr}$. Actually,

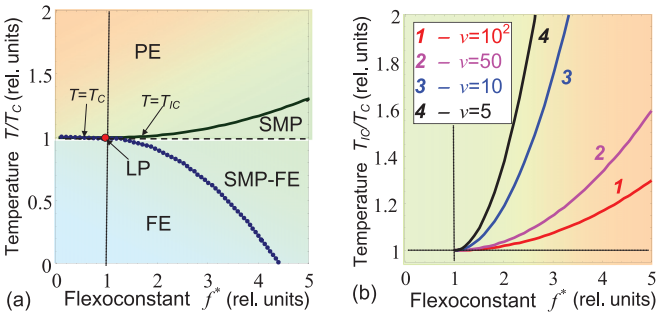

FIG. 1. (a) Phase diagram in coordinates "relative temperature T/T_C – absolute value of dimensionless flexoconstant $f^* = |f|/\sqrt{cg}$" calculated for $v = 10^{-7}$ V s^2/m^2 and other parameters corresponding to the solid solution $Sn_2P_2(S,Se)_6$ (listed in Table SI of the Supplemental Material [67]). The boundaries between the PE, homogeneous FE, and incommensurate SMP that gradually tends to the homogeneous FE phase via partially polar modulated phase (SMP-FE) are shown by solid, dashed, and dotted curves, respectively. Red circle indicates the LP, where the PE, FE, and SMP phases coexist. (b) Dependence of the SMP transition temperature T_{IC}/T_C on the dimensionless flexoconstant f^* calculated for different v values, $v = 100$ (red curve 1), $v = 50$ (magenta curve 2), $v = 10$ (blue curve 3), and $v = 5$ in 10^{-9} V s^2/m^2 (black curve 4).

the condition $\omega^2 = 0$ in Eq. (5) leads to the biquadratic equation for $k_{cr}^2[(\alpha_S + gk_{cr}^2)(vk_{cr}^2 + c) - f^2k_{cr}^2 - 4q^2P_S^2] = 0$. Except for the trivial solution $k_{cr} = 0$, the biquadratic equation has four roots $k_{cr} = \pm k_{1,2}^{cr}$, where

$$k_{1,2}^{cr} = \sqrt{\frac{c}{2v}\left[Q(f) \mp \sqrt{Q^2(f) - 4\frac{v}{cg}\left(\alpha_S - 4\frac{q^2}{c}P_S^2\right)}\right]}. \tag{6}$$

Subscripts "1" and "2" correspond to the signs "−" and "+" before the radical, respectively. The function $Q(f) = \frac{f^2}{cg} - 1 - \frac{\alpha_S v}{cg}$.

Both roots in Eqs. (5) and (6) are real and so exist under the condition $|f| > f_{cr}$, where the temperature-dependent critical value f_{cr} is given by expression

$$|f_{cr}(T)| = \sqrt{\alpha_S(T)v + cg + 2\sqrt{cgv\left[\alpha_S - 4\frac{q^2}{c}P_S^2(T)\right]}}. \tag{7}$$

Under the condition $|f| = f_{cr}$, both roots for the **A** mode in Eq. (5) coincide, $k_1^{cr} = k_2^{cr} = k_0^{cr}$ and $\omega(k_0^{cr}) = 0$, where the critical value is given by the expression $k_0^{cr} = \sqrt{cQ(f)/2v}$.

B. Flexocoupling-induced SMPs

The critical point $\omega_2(k_0^{cr}) = 0$ corresponds to the system transition at temperature $T = T_{IC}$ from the PE phase into the incommensurate SMP with polarization $P(x) = \delta P_1 \sin(k_1^{cr}x) + \delta P_2 \sin(k_2^{cr}x)$ that gradually tends to the homogeneous FE phase with temperature decrease to $T = T_C$ [see Ref. [51] and the regions of PE and SMP in Fig. 1(a)]. Under the condition $P_S^2 = 0$, that is valid in the PE phase at the onset

of SMP, the coefficient $\alpha_S = \alpha_T(T_{IC} - T_C)$, and so the critical value is $k_0^{cr} \sim (T_{IC} - T_C)^{1/4}$. Three phases (PE, FE, and SMP) coexist at the flexocoefficient value $|f| = \sqrt{cg}$, that is a formal analog of a LP [Fig. 1(a)].

The transition temperature from PE to the SMP T_{IC} can be found from the condition $B(k_0^{cr}, T_{IC}) = 0$ (see Appendix A in the Supplemental Material [67]). The solution of the equation exists at flexocoefficients $|f| > \sqrt{cg}$ and has the form

$$T_{IC}(f) = \begin{cases} T_C + \frac{(|f| - \sqrt{cg})^2}{\alpha_T v}, & |f| > \sqrt{cg} \\ \text{absent}, & |f| < \sqrt{cg} \end{cases}. \quad (8)$$

The expression in Eq. (8) shows how the transition temperature $T_{IC}(f)$ to the SMP depends on the flexocoupling constant f and the strain gradient constant v [see Fig. 1(b)].

Also, we predict that the incommensurate modulation of polarization $P(x) = P_0(T) + \delta P_1 \sin(k_1^{cr} x) + \delta P_2 \sin(k_2^{cr} x)$ can appear at temperatures below T_C and high enough flexocoefficients $|f| > \sqrt{cg}$ in the initially commensurate FE [see the region of SMP-FE in Fig. 1(a)]. The only physical reason for the SMP-FE existence is the flexocoupling in the considered case, since we impose the condition $g > 0$ and do not include the gradient term proportional to $w(\partial^2 P/\partial x^2)^2$. However, we included the higher term γP^6, keeping in mind that the strength γ can strongly affect the SMPs stability via the higher harmonics and modulation pattern nonlinearities [68,69]. The analytical expression for the transition temperature from incommensurate SMP-FE to commensurate homogenous FE is absent, so that the diffuse boundary between the phases can be found numerically from the minimum of the free energy in Eq. (2).

Let us consider some additional remarks about the phase diagram depicted in Fig. 1(a). The superposition of SMP and FE was named "rippled phases", and it was regarded to appear in the incommensurate ferroics of type I (see, e.g., Refs. [27,28,62]). In fact, the existence of the SMP-FE in the incommensurate ferroics of type I (corresponding to the second-order phase transition from almost solitonic incommensurate SMP to FE in incipient FEs, like K_2SeO_4) or in the type II (corresponding to the first-order phase transition from almost sinusoidal incommensurate SMP to FE in proper FEs, like $Sn_2P_2(Se_xS_{1-x})_6$ family [70]) can be crucial for our model verification, since our prediction of SMP-FE is based on the flexocoupling impact only.

C. Soft acoustic mode behavior in the vicinity of critical wave vectors

As a next step, let us expand the frequency $\omega(k)$ of the **A** mode given by Eq. (5) in a series in the vicinity of critical values $k \to \pm k_{1,2}^{cr}$ and $k \to k_0^{cr}$

$$\omega\left(k \to k_1^{cr} - 0\right) \approx \frac{\sqrt{2gv\left(k_1^{cr}\right)^3 \left|\left(k_1^{cr}\right)^2 - \left(k_2^{cr}\right)^2\right|}\sqrt{k_1^{cr} - k}}{\sqrt{\alpha_S \rho + \left(k_1^{cr}\right)^2 (c\mu + g\rho - 2fM) + \mu v \left(k_1^{cr}\right)^4}}, \quad (9a)$$

$$\omega\left(k \to k_2^{cr} + 0\right) \approx \frac{\sqrt{2gv\left(k_2^{cr}\right)^3 \left|\left(k_1^{cr}\right)^2 - \left(k_2^{cr}\right)^2\right|}\sqrt{k - k_2^{cr}}}{\sqrt{\alpha_S \rho + \left(k_2^{cr}\right)^2 (c\mu + g\rho - 2fM) + \mu v \left(k_2^{cr}\right)^4}}, \quad (9b)$$

$$\omega\left(k \to k_0^{cr}\right) \approx \frac{2\sqrt{gv}\left(k_0^{cr}\right)^2 \left|k - k_0^{cr}\right|}{\sqrt{\alpha_S(T)\rho + (c\mu + g\rho - 2fM)\left(k_0^{cr}\right)^2 + \mu v \left(k_0^{cr}\right)^4}}. \quad (9c)$$

For derivation of Eq. (9), see Appendix B in the Supplemental Material [67]. The difference $|(k_1^{cr})^2 - (k_2^{cr})^2| \equiv |\frac{\alpha_S v + cg - f^2}{gv}|$ in accordance with the Vieta theorem. Note that an addition of higher order terms proportional to $\frac{w}{2}(\frac{\partial^2 P}{\partial x^2})^2$ in the free energy in Eq. (1) changes the difference between k_1^{cr} and k_2^{cr}, since $gv \to (gv + cw)$ in the denominator of the difference $|(k_1^{cr})^2 - (k_2^{cr})^2|$ (see also eq. (10) in Ref. [51]). However, the "gap" between k_1^{cr} and k_2^{cr} remains for reasonable values of parameter $w > 0$ (see Fig. 3(c) in Ref. [51] and compare with Fig. 8(a) in Ref [16].). We consider the case $w = 0$ in this paper, since for the most commensurate FEs, the value and sign of w is unknown.

Figure 2 illustrates that the frequency of the **A** mode is independent on the flexocoupling at very small k, namely $\omega(k) \cong (\sqrt{c/\rho})k$ in accordance with Eq. (5). If the inequality $|f| \ll f_{cr}$ is valid, the **A** mode frequency is equal to zero at $k = 0$ only, and it monotonically increases as k increases (curve 1). As f increases in the range $f_{inf}(T) < |f| < f_{cr}(T)$, the **A** mode frequency is zero at $k = 0$ only, but then the local minimum appears at $k = k_{min}$ (curve 2).

Under the condition $|f| = f_{cr}$, the **A** mode frequency is also zero at $k = k_0^{cr}$ (namely, its graph touches the k axis, see curve 3), where k_0^{cr} is given expression $k_0^{cr} = \sqrt{cQ(f)/2v}$. Under the condition $|f| > f_{cr}$, the **A** mode frequency is positive in the regions $0 < k < k_1^{cr}$ and $k > k_2^{cr}$; it is zero at $k = 0$, $k = k_1^{cr}$, and $k = k_2^{cr}$; and it does not exist in the region $k_1^{cr} < k < k_2^{cr}$ (curve 4), so that the square root laws $\omega(k) \sim \sqrt{k_1^{cr} - k}$ and $\omega(k) \sim \sqrt{k - k_2^{cr}}$ are valid in the vicinity of critical values $k \to k_1^{cr} - 0$ and $k \to k_2^{cr} + 0$, respectively (see dashed curves).

Analyzing the results shown in Fig. 2 for the case $|f| > f_{cr}$, one should ask two reasonable questions: What happens in a FE if the spatial fluctuations of the wave vector k are within the range $k_1^{cr} \leqslant k \leqslant k_2^{cr}$? Are there any experiments that reveal the "softening" of the **A** mode similar to the ones shown by the curves 2, 3, and 4 in Fig. 2?

The answer to the first question is quite simple. Using the results of Refs. [50,51], the SMP with the modulation vectors

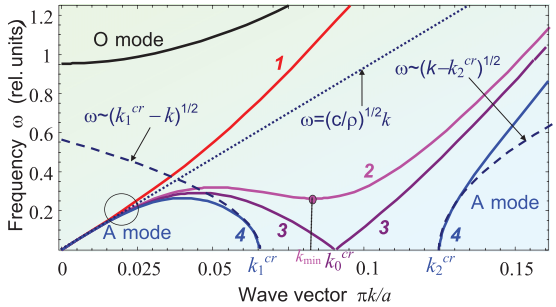

FIG. 2. Dependences of the phonon frequency ω^* on the wave vector $k^* = ak/\pi$. The lattice constant is a. **O** mode (black curve) is not sensitive to the f value for small k. **A**-mode curves calculated at $f = 0$ (red curve 1), $|f| = 0.5 f_{cr}$ (magenta curve 2), $|f| = f_{cr}$ (dark violet curve 3), and $|f| \approx 1.1 f_{cr}$ (blue curve 4) are shown. Dotted curve is the linear approximation $\omega(k) \cong (\sqrt{c/\rho})k$, dashed curves show are square root approximations from Eqs. (9a) and (9b), respectively (see Appendix B in the Supplemental Material [67]).

$k = k_1^{cr}$ and $k = k_2^{cr}$ can occur in the temperature range for which $|f| > f_{cr}(T)$. In essence, this means that any fluctuation having a wave vector in the interval $k_1^{cr} \leqslant k \leqslant k_2^{cr}$ relaxes in a short time to the value $k = k_1^{cr}$ or to $k = k_2^{cr}$ (which is less probable, since the larger the wave vector is, the greater the influence of the lattice anharmonicity on the phonon spectrum is, and so the less applicable the linear approximation for the perturbations of $\tilde{P}$ and $\tilde{u}$ are). In this sense, acoustic vibrations with wave vectors $k_1^{cr} < k < k_2^{cr}$ are absent in the lattice, so the frequency of the corresponding **A** mode is absent in this interval of wave vectors. The "normal" **A** mode exists in the interval $0 < k < k_1^{cr}$ and $k > k_2^{cr}$; it softens approaching the point $k = k_1^{cr}$, as well as at $k = k_2^{cr}$. On the other hand, following the idea that, owing to the mode-mode coupling, at some temperature, the transverse **A** mode gets unstable and triggers the appearance of an incommensurate phase [12]. The simulation of the dispersion relations in the range of wave vectors $k_1^{cr} < k < k_2^{cr}$ at certain temperature values requires a consistent consideration of the fact that there is a stable SMP in this region. The latter must substantially affect the nature of the solutions of the linearized equations [27,68,69]. Unfortunately, the linear theory we developed does not allow any quantitative predictions about the properties of the nonlinear solutions in the SMP region.

The answer to the second question is not simple because the value of the flexocoefficient f is fixed for each specific FE, and in a general case, it is relatively weakly dependent on the temperature, and so one cannot vary it within the necessary limits in order to "get into" the interval $|f| > f_{cr}(T)$. However, experimentalists have all the possibilities to measure phonon spectra in a wide range of temperatures, corresponding to variable $f_{cr}(T)$ that essentially depends on temperature, primarily due to the temperature dependence of $\alpha_S(T)$ according to Eq. (4). In particular, $\alpha_S(T)$ depends linearly on the temperature in the PE phase $\alpha_S(T) = \alpha_T(T - T_C)$. Thus, the form of the acoustic branch can be changed similarly to the changes shown in Fig. 2, by changing only the temperature for an arbitrary value of the flexocoefficient f. A typical scenario is shown in Fig. 3(a), where the dimensionless parameter $\alpha_S^*(T) = \alpha_T^*[(T/T_C) - 1]$ is introduced, where $\alpha_T^* = v\alpha_T T_C/(gc)$ is the dimensionless stiffness constant; $k^* = ak/\pi$ is the dimensionless wave vector, a is the lattice constant. The dependence $\omega(k)$ shows only a very small bend for the highest relative temperature $\alpha_S^* = 1.5$ (curve 4). With the temperature decrease corresponding to the value of $\alpha_S^* = 1.0$, a local minimum appears instead of the bend, which becomes deeper and noticeable as α_S decreases (curve 3). With a further decrease in temperature to a critical value of $\alpha_S^* = 0.9$ (that corresponds to the temperature of the SMP transition $T = T_{IC}$), the zero point $\omega(k) = 0$ arises at $k = k_0^{cr}$ (curve 2). Finally, the "dip" occurs on the acoustic branch in the wave vector interval $k_1^{cr} < k < k_2^{cr}$ at $\alpha_S^* = 0.8$ (see curve 1) corresponding to the appearance of SMP in a certain temperature interval $T < T_{IC}$.

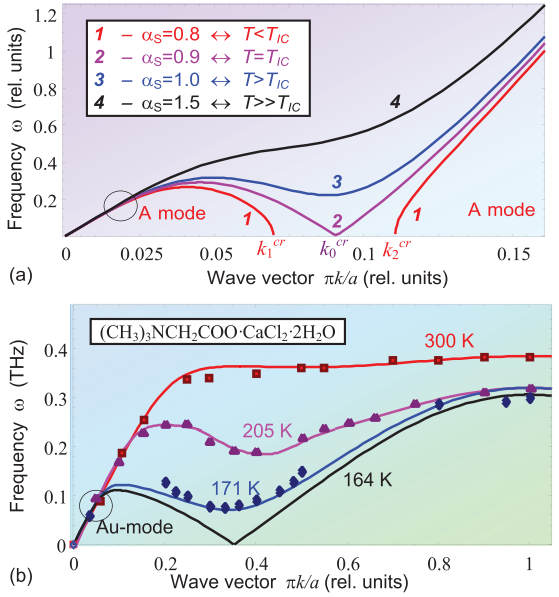

FIG. 3. (a) Dependences of the **A**-mode frequency ω^* on the wave vector $k^* = ak/\pi$. The curves calculated for fixed parameters $f^* = 1.98$, $M^* = 0.1$, $\mu^* = 0.05$, and different temperatures, which corresponds to different $\alpha_S^* = 0.8$ (red curve 1), $\alpha_S^* = 0.9$ (magenta curve 2), $\alpha_S^* = 1.0$ (blue curve 3), and $\alpha_S^* = 1.5$ relative units (black curve 4). (b) Acoustic phonon spectra measured experimentally in incommensurate organic FE $(CH_3)_3NCH_2COO{\cdot}CaCl_2{\cdot}2H_2O$ (symbols from Refs. [9,57]) and calculated at 300, 205, 171, and 164 K (solid curves). Experimental data for 164 K is absent. Fitting parameters are Curie temperature $T_C = 125$ K, stiffness constant $\alpha_T^* \approx 1$ in the coefficient $\alpha_S^* = (T) = \alpha_T^*[(T/T_C) - 1]$, static and dynamic flexocoupling constants $f^* \approx 1.280$ and $M^* = 0.095$, $\mu^* = 0.3$, and amplitude $\omega_0 = 3 \times 10^{12}$ s^{-1}.

Following Ref. [51], the dimensionless variables and parameters, which were used in Figs. 1 –3, are described in Appendix A in the Supplemental Material [67]. The dimensionless stiffness constant $\alpha_T^* = v\alpha_T T_C/(gc)$ and temperature T/T_C are not the sole parameters which control the **A** mode frequency behavior. Another important parameter is the dimensionless static flexoconstant $f^* = |f|/\sqrt{cg}$ that controls the values $k_{1,2}^{cr}$ as well as the k scale, i.e. the saturation rate of $\omega(k)$ [see Fig. 2]. At fixed f, the dimensionless dynamic flexoconstant $M^* = cM/(2\rho f)$ strongly affects the **A** mode behavior starting from small k^*, since the increase of $|M^*|$ leads to the noticeable changes of the frequency value and

its slope at $k^* \geqslant 0.05$ (see Fig. S1(a) in the Supplemental Material [67]). The increase is monotonic at $fM < 0$, and nonmonotonic for $fM > 0$ (compare dashed and solid curves in Fig. S1(a) in the Supplemental Material [67]). The pole at $M^2 = \mu\rho$ exists for the **O** mode only; for the **A** mode, it cancels as a virtual one [see Eqs. (5)]. The increase of the strain-gradient coefficient v leads to the same effect as the increase of temperature (see Fig. S1(b) in the Supplemental Material [67]) because $\alpha_S^*(T) \sim v[(T/T_C) - 1]$. The change of the parameter $\mu^* = c\mu/(2g\rho)$ affects the **A**-mode frequency spectrum relatively weakly. Being positive for $g > 0$ and typically small μ^* affects the saturation value of the **A** mode frequency. The saturation value decreases 2–10 times as μ^* increases (10–100) times. The dimensionless frequency amplitude is given by the expression $\omega_0 = c/\sqrt{4v\rho}$ that is about 3 THz for chosen parameters. A rigorous analysis of the **A**-mode frequency dependence on all these parameters can be done using the analytical expression in Eq. (5) and its series expansion in Eq. (9). Since it depends on the parameters fixed for a particular problem, and on the ones varying, we defer the cumbersome task to future studies.

An analysis of the available experimental data has shown that the anomalous flattening, bends, inflections, minima, and maxima in the **A**-mode frequency spectra $\omega(k)$ are observed experimentally at $k \sim (0.2 - 0.4)\pi/a$ quite often [6,9,16,59], and are explained by the interaction of optical and acoustic modes in proper FEs [57], as well as by electron-density multiphonon interactions in incipient FEs [20]. For example, from the experimental data shown in Fig. 3(b), it can be seen that the bend on the lowest acoustic **A** mode is absent at 300 K in organic FE $(CH_3)_3NCH_2COO{\cdot}CaCl_2{\cdot}2H_2O$. A noticeable minimum appears even at 205 K, and the softening of the **A** mode continues at 171 K. The true incommensurate phase occurs at 164 K and coexists with commensurate FE phase from $T_C = 125$ K up to 43 K according to the "devil staircase" scenario [9]. However, the experimental scenario [9] agrees semiquantitatively with the theoretical one shown in Fig. 3(a). To illustrate this, we add solid curves for the **A** mode calculated from Eq. (5) for the temperatures (300–164) K in Fig. 3(b). One can see the agreement between theoretical curves and experimental points.

However, the "true" soft **A** modes, which are absent at $k_1^{\rm cr} < k < k_2^{\rm cr}$, have not been observed so far, although the absence of the **A** mode in proper and incipient FEs at definite k-range is possible in a number of microscopic theories (see, e.g., Fig. 6(b) for organic FE $(CH_3)_3NCH_2COO{\cdot}CaCl_2{\cdot}2H_2O$ in Ref. [57], Fig. 2 for $SrTiO_3$ in Ref. [23], and Fig. 8(a) for $Sn_2P_2(Se_{0.28}S_{0.72})_6$ in Ref. [16]). It is also quite possible that the value $f_{\rm cr}(T)$ is not reached for some real materials, or the range of critical values $k_1^{\rm cr} < k < k_2^{\rm cr}$ goes beyond the region of the linear model applicability. The possibility of other reasons (originated mainly from the modes interaction) cannot be excluded (see, e.g., Ref. [19]).

Also, we should note that Perez-Mato [71] performed the symmetry analysis of the phase transition sequence in $(CH_3)_3NCH_2COO{\cdot}CaCl_2{\cdot}2H_2O$ using the theory of irreproducible representations for the *Pnma* point group of its structural order parameter Q. Unfortunately, the results [71] do not contain a direct way to express polarization components P_i via Q and Q^*, and so this may impose symmetry

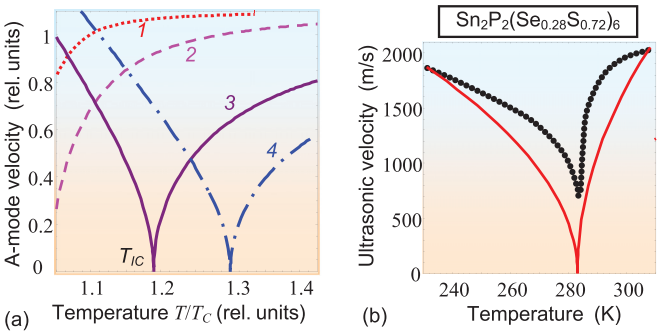

FIG. 4. (a) Temperature dependences of the acoustic mode velocity $V(T)$ calculated at $f = 0$ (red curve 1), $|f| = 0.5 f_{\rm cr}$ (magenta curve 2), $|f| = f_{\rm cr}$ (dark violet curve 3), and $|f| \approx 1.25 f_{\rm cr}$ (blue curve 4). (b) Experimental temperature dependence of shear XZ ultrasonic mode velocity (x displacement in z direction of propagation) near the LP in $Sn_2P_2(Se_{0.28}S_{0.72})_6$ crystal (circles from Ref. [16]) and calculated $V(T)$ at $|f| = f_{\rm cr}$ (solid curve).

limitations of the Lifshitz invariant in the continuous medium approximation.

Another limitation is that we used as a one component approximation $\frac{f}{2}(P\frac{\partial u}{\partial x} - u\frac{\partial P}{\partial x})$ of the tensorial Lifshitz invariant $\frac{f_{klij}}{2}(P_i\frac{\partial u_{kl}}{\partial x_j} - u_{kl}\frac{\partial P_i}{\partial x_j})$, containing several terms which were nonzero for all point symmetry groups, including *Pnma*. For the *Pnma* group, the tensor of flexoelectric coupling f_{klij} has the form listed at the end of Appendix A in the Supplemental Material [67]. The result was obtained using the direct matrix method adopted by Eliseev *et al.* [37,72,73] for the tensors of flexomagnetic, flexomagnetoelectric, and piezomagnetic couplings.

Hence, the question is whether it is correct leaving the only one term $\frac{f}{2}(P\frac{\partial u}{\partial x} - u\frac{\partial P}{\partial x})$ from the full tensorial invariant, since the fluctuations of polarization and strain can be nonzero for several polarization components and directions of the wave vector. However, we can argue that we used the flexoelectric term allowed by arbitrary symmetry (up to the symmetry of an isotropic body) without claiming a quantitative description of the dispersion relations for $(CH_3)_3NCH_2COO{\cdot}CaCl_2{\cdot}2H_2O$ for an arbitrary direction of the wave vector.

Note that Patel *et al.* [74] developed an *ab initio* model predicting the phase transition dynamics of antipolar cation phonon modes towards the *Pnma* phase and revealed that some antipolar phonons are rather soft in the phase. The effect can originate in $BiFeO_3$ from a specific trilinear energetic coupling between antipolar cation phonons and fluctuations of oxygen octahedral tiltings.

D. Elastic softening of the sound velocity

Let us discuss the indirect evidences of the **A**-mode softening in the FEs with incommensurate SMP. The phase velocity of the acoustic wave is given by the expression $V(k) = |\omega|/k$. Temperature dependences of the **A**-mode velocity calculated for different values of flexoconstant and temperatures $T > T_C$ ($\alpha_S^* > 0$) are shown in Fig. 4(a). The velocity monotonically increases and saturates as T increases at $f = 0$ and $|f| < f_{\rm cr}$ (curves 1–2), the pronounced minima at $T = T_{\rm IC}(f)$ appear

at $|f| \geqslant f_{cr}$, and the values of $T_{IC}(f)$ increase as f increases (curves 3–4).

The sound velocity can be measured in FEs by Brillouin scattering and the ultrasonic pulse-echo method [16,11,14,18]. In particular, the temperature dependencies of sound velocity and attenuation were measured by these methods in proper uniaxial $Sn_2P_2(Se_xS_{1-x})_6$ FEs in the vicinity of LP ($x = 0.28$ and $T_{LP} = 284$ K) [16,18]. The pronounced softening of the **A** mode, manifesting itself as remarkable lowering of hypersound velocity for the TA phonons that are polarized in crystallographic plane containing the vector of spontaneous polarization and the wave vector of modulation, was observed [see Fig. 4(b)]. It was shown that elastic softening in the hypersound range is induced mostly by linear interaction between soft optic and acoustic phonon branches [16].

E. Temperature dependence of static dielectric susceptibility

Let us analyze the temperature dependence of the static dielectric susceptibility that follows from Eqs. (3)–(6). The temperature-dependent k spectrum of the static dielectric susceptibility $\tilde{\chi}(k,\omega = 0,T)$ can be represented in the form

$$\tilde{\chi}(k,0,T) = \begin{cases} \frac{vk^2+c}{gv\left[k^2-\left(k_0^{cr}\right)^2\right]^2}, & T = T_{IC}, \quad k_{1,2}^{cr} = k_0^{cr} \equiv \sqrt[4]{\frac{c\alpha_T(T_{IC}-T_C)}{4vg}} \\ \frac{vk^2+c}{gv\left\{k^2-\left[k_1^{cr}(T)\right]^2\right\}\left\{k^2-\left[k_2^{cr}(T)\right]^2\right\}}, & T \neq T_{IC}, \quad k_1^{cr}(T) \neq k_2^{cr}(T). \end{cases} \tag{10}$$

Derivation details of Eq. (10) are given in Appendix C of the Supplemental Material [67].

The x-dependent static susceptibility $\chi(x,0,T)$ can be obtained after inverse Fourier transformations of the spectrum in Eq. (10), whose results depend on the temperature via the properties of $k_1^{cr}(T)$ and $k_2^{cr}(T)$ [see Eq. (C2)]. The average susceptibility of a bulk FE $\langle\chi(x,0,T)\rangle = \int_{-\infty}^{\infty} dx\,\chi(x,0,T)$ can be derived from Eq. (10) in the temperature ranges of PE ($T > T_{IC}$) and homogeneous FE ($T < T_C$) phases [see Eq. (C3)]. In the SMP phase ($T_C < T < T_{IC}$), the integral $\int_{-\infty}^{\infty} dx\,\chi(x,0,T)$ does not exist is the sense of normal convergence, and it was substituted by the integration $\int_{-2L}^{2L} dx\,\chi(x,0,T)$ followed by the averaging of the oscillated functions over the size $L \to \infty$. The average static susceptibility obtained by the way has the form

$$\langle\langle\chi(T)\rangle\rangle \cong \begin{cases} \frac{1}{\alpha_T(T-T_C)+3\beta^* P_S^2(T)+5\gamma P_S^4(T)}, & T \leqslant T_C \\ \frac{1}{\alpha_T(T-T_C)+3\beta^*\delta P^2(T)+5\gamma\delta P^2(T)}, & T_C < T \leqslant T_{IC} \\ \frac{1}{\alpha_T(T-T_C)}, & T > T_{IC}. \end{cases} \tag{11}$$

where $P_S^2 = \frac{1}{2\gamma}[\sqrt{\beta^{*2} - 4\gamma\alpha_T(T-T_C)} - \beta^*]$ is the square of spontaneous polarization that is homogeneous and stable at temperatures lower than Curie temperature $T \leqslant T_C$.The spontaneous polarization appears at $T = T_C$ in accordance with the law $P_S^2 \sim (T_C - T)$.

The transition temperature to the SMP phase $T_{IC}(f^*)$ exists at $f^* > 1$ and depends on the flexoconstant f^* in accordance with Eq. (8), namely $T_{IC}(f^*) = T_C[1 + \frac{(f^*-1)^2}{\alpha_T^*}]$.

The function $\delta P^2(T)$ is the mean square value of the polarization modulation existing in SMP at $T_C < T \leqslant T_{IC}$. It should be found from the free energy in Eq. (1) minimization in a self-consistent manner allowing for the nonlinear terms (see, e.g., Refs. [27,68,69]). The temperature dependence of δP^2 in the vicinity of $T = T_{IC}$ is $\delta P^2(T) \cong \delta P_0^2(1 - \frac{T}{T_{IC}})$, where the temperature-dependent function δP_0^2 is nonzero at $T = T_{IC}$. At $T \leqslant T_C$, the function $\delta P^2(T)$ can either disappear at once [according to the scenario of the second-order phase transition for $P_S(T) \sim \sqrt{T_C - T}$], or firstly becomes metastable $T = T_C$ and then unstable with the temperature decrease below T_C [more close to the first-order scenario for $P_S(T)$], leading to the coexistence region of FE and SMP phases, shown in Fig. 1(a). The metastability of SMP should lead to the pronounced temperature hysteresis of the dielectric susceptibility, but its quantitative description is beyond the scope of this paper.

Solid curves in Figs. 5(a) and 5(b) illustrate the temperature dependences of direct and inverse average static susceptibility

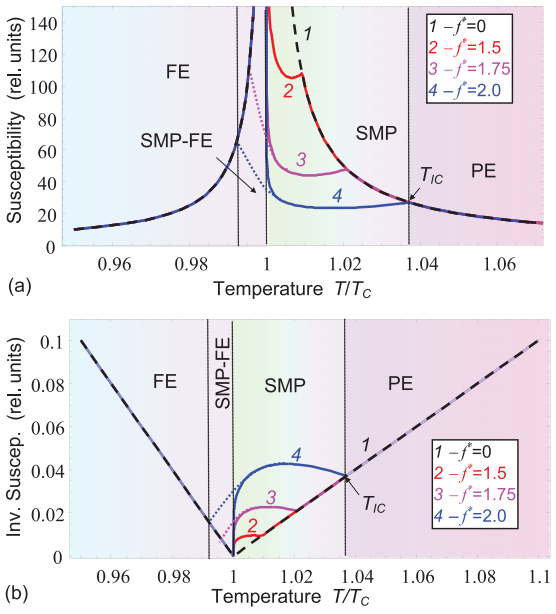

FIG. 5. Temperature dependence of the (a) direct and (b) inverse static dielectric susceptibility for a FE with the second-order phase transition at T_C calculated for different flexocoupling constants $f^* = 0$ (dashed black curve 1), 1.5 (red curve 2), 1.75 (magenta curve 3), and 2.0 (blue curve 4); $v = 5 \times 10^{-8}$ V s^2/m^2 and other parameters corresponding to $Sn_2P_2S_6$ (listed in Table SI the Supplemental Material [67]).

calculated from Eq. (11) for the FE with the second-order phase transition at $T = T_C$ (corresponding to $\beta^* > 0$ and $\gamma \geqslant 0$) at different flexocoupling constants f^*. Dashed black curves corresponding to $f^* = 0$ are the reference curves, which in fact are conventional Curie-Weiss dependences. The dependences of averaged direct and inverse susceptibility do not change from the ones calculated at $f^* = 0$ until $|f^*| < f^*_{\rm cr}$. Solid curves corresponding to $|f^*| > f^*_{\rm cr}$ have the specific features (maxima or fracture) at $T = T_{\rm IC}(f^*)$ which become more pronounced as f^* increases [compare solid curves 2, 3, and 4 in Fig. 5]. The interval of SMP stability increases as f^* increases from 1.5 to 2; the result is in accordance with Eq. (9).

Note that the existence of a fracture or a maximum at $T = T_{\rm IC}$ is a characteristic feature of SMP transition [55,70], and so the solid curves 2–4 in Fig. 5(a) look similar to the black curves (cooling) shown in Figs. 1(f) and 1(g) in Ref. [70]. However, the description of pronounced temperature hysteresis of dielectric susceptibility revealed in Ref. [70] is beyond the scope of our model. Actually, we calculated the solid curves in Fig. 5 using the specific temperature dependence of the amplitude $\delta P^2(T)$ in the SMP and regarding it independent on the direction of the temperature change (heating or cooling). Due to this, the amplitude $\delta P^2(T)$ is zero at $T = T_{\rm IC}$ (as it should be for the type II SMP), then it increases and reaches a maximum in the interval $T_C < T < T_{\rm IC}$, and then becomes zero at temperature $T = T_C$, when the homogeneous FE polarization P_S appears according to the law $P_S(T) \sim \sqrt{T_C - T}$. As a consequence, the susceptibility has a feature at $T = T_{\rm IC}$ and diverges at $T = T_C$.

However, the coexistence of SMP and FE is absent for the solid curves. In other words, solid curves in Fig. 5 do not reflect the possible coexistence of the metastable SMP with the absolutely stable FE below T_C [shown in Fig. 1(a)]. For the first-order scenario of P_S appearance at $T = T_C$, $P_S^2(T \to T_C) = \frac{-\beta^*}{\gamma}$ realized in the case $\beta^* < 0$ and $\gamma > 0$, the temperature dependence of $\delta P^2(T)$ should be different, leading to another form of the dielectric susceptibility temperature dependence. Actually, for the FE with the first-order phase transition at $T = T_C$ (corresponding to the case $\beta^* < 0$ and $\gamma > 0$), the temperature dependences of the dielectric susceptibility in the existing SMP-FE region have the form shown schematically by the dotted curves in Figs. 5(a) and 5(b).

IV. CONCLUSIONS

Using the LGD theory and one component approximation, we derived analytical expressions for the singular points (zeros, breaks, etc.) of the phonon **A**-mode frequency $\omega(k)$ dependent on the wave vector k and examined the conditions of the soft acoustic modes appearance in FEs depending on the magnitude of the flexoelectric coefficient f and temperature T of the FE.

If the magnitude of the flexocoefficient f is equal to the temperature-dependent critical value $f^{\rm cr}(T)$ at the temperature $T = T_{\rm IC}$, $|f| = f^{\rm cr}(T_{\rm IC})$, then the **A**-mode frequency tends to zero at $k \to k_0^{\rm cr}$ according to the linear law $\omega(k \to k_0^{\rm cr}) \sim |k - k_0^{\rm cr}|$, and the FE polarization becomes spatially modulated.

When the magnitude of the flexocoefficient is more than the critical value $|f| > f^{\rm cr}(T)$ in a temperature range $T_C < T < T_{\rm IC}$ corresponding to the incommensurate SMP, the **A** mode becomes zero for two wave vectors $k = k_{1,2}^{\rm cr}$ according to the square root law $\omega(k \to k_{1,2}^{\rm cr}) \sim \sqrt{|k_{1,2}^{\rm cr} - k|}$ and does not exist in the range of wave vectors $k_1^{\rm cr} < k < k_2^{\rm cr}$. At fixed flexocoefficient f, the transition into the SMP can appear at the temperature $T_{\rm IC}$ that depends on f as $T_{\rm IC}(f) - T_C \sim (|f| - \sqrt{cg})^2$, where T_C is the FE Curie temperature.

The available experimental data on neutron scattering in organic FE $(CH_3)_3NCH_2COO{\cdot}CaCl_2{\cdot}2H_2O$ [9] are in a semiquantitative agreement with our theoretical results. For improvement and for quantification of the theory, it is necessary to measure the frequency dependence of the **A** mode in a uniaxial FE with a SMP in the temperature interval near its occurrence. In addition, we predicted the appearance of the "rippled" flexocoupling-induced SMP-FE phase in the initially commensurate ferroics.

Finally, the temperature dependence of dielectric susceptibility in the incommensurate SMP phase was calculated, and the feature (maximum or fracture) at incommensurate phase transition temperature is in agreement with experiments for many ferroics with SMPs [55,70].

ACKNOWLEDGMENTS

The authors express their gratitude to the referees for valuable suggestions and useful discussions. A.N.M. and E.A.E. acknowledge the Center for Nanophase Materials Sciences (Grant No. CNMS2016-061).

[1] M. E. Lines and A. M. Glass, *Principles and Application of Ferroelectrics and Related Materials* (Clarendon Press, Oxford, 1977).

[2] W. Cochran, Crystal Stability and the Theory of Ferroelectricity, Phys. Rev. Lett. **3**, 412 (1959).

[3] G. Shirane, J. D. Axe, J. Harada, and J. P. Remeika, Soft ferroelectric modes in lead titanate, Phys. Rev. B **2**, 155 (1970).

[4] W. Cochran, Dynamical, scattering and dielectric properties of ferroelectric crystals, Adv. Phys. **18**, 157 (1969).

[5] J. D. Axe, J. Harada, and G. Shirane, Anomalous acoustic dispersion in centrosymmetric crystals with soft optic phonons, Phys. Rev. B **1**, 1227 (1970).

[6] G. Shirane and Y. Yamada, Lattice-dynamical study of the 110 K phase transition in $SrTiO_3$, Phys. Rev. **177**, 858 (1969).

[7] R. Currat, H. Buhay, C. H. Perry, and A. M. Quittet, Inelastic neutron scattering study of anharmonic interactions in orthorhombic $KNbO_3$, Phys. Rev. B **40**, 10741 (1989).

[8] I. Etxebarria, M. Quilichini, J. M. Perez-Mato, P. Boutrouille, F. J. Zuniga, and T. Breczewski, Inelastic neutron scattering investigation of external modes in incommensurate and commensurate A_2BX_4 materials, J. Phys.: Condens. Matter **4**, 8551 (1992).

[9] J. Hlinka, M. Quilichini, R. Currat, and J. F. Legrand, Dynamical properties of the normal phase of betaine calcium chloride dihydrate. I. Experimental results, J. Phys.: Condens. Matter **8**, 8207 (1996).

[10] J. Hlinka, S. Kamba, J. Petzelt, J. Kulda, C. A. Randall, and S. J. Zhang, Origin of the "Waterfall" Effect in Phonon Dispersion of Relaxor Perovskites, Phys. Rev. Lett. **91**, 107602 (2003).

[11] V. Goian, S. Kamba, O. Pacherova, J. Drahokoupil, L. Palatinus, M. Dusek, J. Rohlıcek, M. Savinov, F. Laufek, W. Schranz, A. Fuith, M. Kachlık, K. Maca, A. Shkabko, L. Sagarna, A. Weidenkaff, and A. A. Belik, Antiferrodistortive phase transition in $EuTiO_3$, Phys. Rev. B **86**, 054112 (2012).

[12] A. K. Tagantsev, K. Vaideeswaran, S. B. Vakhrushev, A. V. Filimonov, R. G. Burkovsky, A. Shaganov, D. Andronikova, A. I. Rudskoy, A. Q. R. Baron, H. Uchiyama, D. Chernyshov, A. Bosak, Z. Ujma, K. Roleder, A. Majchrowski, J.-H. Ko, and N. Setter, The origin of antiferroelectricity in $PbZrO_3$, Nat. Commun. **4**, 2229 (2013).

[13] J.-W. Kim, P. Thompson, S. Brown, P. S. Normile, J. A. Schlueter, A. Shkabko, A. Weidenkaff, and P. J. Ryan, Emergent Superstructural Dynamic Order due to Competing Antiferroelectric and Antiferrodistortive Instabilities in Bulk $EuTiO_3$, Phys. Rev. Lett. **110**, 027201 (2013).

[14] R. G. Burkovsky, A. K. Tagantsev, K. Vaideeswaran, N. Setter, S. B. Vakhrushev, A. V. Filimonov, A. Shaganov, D. Andronikova, A. I. Rudskoy, A. Q. R. Baron, H. Uchiyama, D. Chernyshov, Z. Ujma, K. Roleder, A. Majchrowski, and J.-H. Ko, Lattice dynamics and antiferroelectricity in PbZrO 3 tested by x-ray and Brillouin light scattering, Phys. Rev. B **90**, 144301 (2014).

[15] J. Hlinka, I. Gregora, and V. Vorlıcek, Complete spectrum of long-wavelength phonon modes in Sn2P2S6 by Raman scattering, Phys. Rev. B **65**, 064308 (2002).

[16] A. Kohutych, R. Yevych, S. Perechinskii, V. Samulionis, J. Banys, and Yu Vysochanskii, Sound behavior near the Lifshitz point in proper ferroelectrics, Phys. Rev. B **82**, 054101 (2010).

[17] A. Kohutych, R. Yevych, S. Perechinskii, and Y. Vysochanskii, Acoustic attenuation in ferroelectric $Sn_2P_2S_6$ crystals, Open Phys. **8**, 905 (2010).

[18] Yu M. Vysochanskii, A. A. Kohutych, A. V. Kityk, A. V. Zadorozhna, M. M. Khoma, and A. A. Grabar, Tricritical behavior of $Sn_2P_2S_6$ ferroelectrics at hydrostatic pressure, Ferroelectrics **399**, 83 (2010).

[19] R. M. Yevych, Yu. M. Vysochanskii, M. M. Khoma, and S. I. Perechinskii, Lattice instability at phase transitions near the Lifshitz point in proper monoclinic ferroelectrics, J. Phys.: Condens. Matter **18**, 4047 (2006).

[20] R. A. Cowley, Lattice dynamics and phase transitions of strontium titanate, Phys. Rev. **134**, A981 (1964).

[21] A. Bussmann-Holder, H. Büttner, and A. R. Bishop, Coexistence of polar order and local domain dynamics in ferroelectric perovskites: the case of $SrTi^{18}O_3$, Ferroelectrics **363**, 73 (2008).

[22] A. Bussmann-Holder, Electron-phonon-interaction-driven anharmonic mode-mode coupling in ferroelectrics: The origin of acoustic-mode anomalies, Phys. Rev. B **56**, 10762 (1997).

[23] A. Bussmann-Holder, H. Buttner, and A. R. Bishop, Polar-Soft-Mode-Driven Structural Phase Transition in $SrTiO_3$, Phys. Rev. Lett. **99**, 167603 (2007).

[24] R. Blinc and B. Zeks, *Soft Mode in Ferroelectrics and Antiferroelectrics* (North-Holland Publishing Company, Amsterdam, 1974).

[25] V. G. Vaks, *Introduction to the Microscopic Theory of Ferroelectrics* (Nauka, Moscow, 1973), in Russian.

[26] A. D. Bruce, R. A. Cowley, and A. F. Murray, The theory of structurally incommensurate systems. II. Commensurate-incommensurate phase transitions, J. Phys. C **11**, 3591 (1978).

[27] V. A. Golovko, An exact solution to the equations of the phenomenological theory of the incommensurate phase, Zh. Eksp. Teor. Fiz. **87**, 1092 (1984).

[28] A. P. Levanyuk, S. A. Minyukov, and A. Cano, Universal mechanism of discontinuity of commensurate-incommensurate transitions in three-dimensional solids: strain dependence of soliton self-energy, Phys. Rev. B **66**, 014111 (2002).

[29] R. M. Hornreich, M. Luban, and S. Shtrikman, Critical Behavior at the Onset of $\vec{k}$-Space Instability on the λ Line, Phys. Rev. Lett. **35**, 1678 (1975).

[30] V. A. Golovko, Exact solutions of equations describing an incommensurate phase in the absence of the Lifshitz invariant, Zh. Eksp. Teor. Fiz. **94**, 182 (1988).

[31] V. S. Mashkevich and K. B. Tolpygo, The interaction of vibrations of nonpolar crystals with electric fields, Zh. Eksp. Teor. Fiz. **31**, 520 (1957).

[32] Sh. M. Kogan, Piezoelectric effect under an inhomogeneous strain and an acoustic scattering of carriers of current in crystals, Solid State Phys. **5**, 2829 (1963).

[33] M. D. Glinchuk, A. V. Ragulya, V. A. Stephanovich, *Nanoferroics* (Springer, Dordrecht, 2013), p. 378.

[34] S. V. Kalinin and A. N. Morozovska, Multiferroics: Focusing the light on flexoelectricity (Comment), Nat. Nanotechnol. **10**, 916 (2015).

[35] *Flexoelectricity in Solids: From Theory to Applications*, edited byA. K. Tagantsev and P. V. Yudin (World Scientific, New Jersey, 2016), Chap. 1.

[36] A. Y. Borisevich, E. A. Eliseev, A. N. Morozovska, C.-J. Cheng, J.-Y. Lin, Y.-H. Chu, D. Kan, I. Takeuchi, V. Nagarajan, and S. V. Kalinin, Atomic-scale evolution of modulated phases at the ferroelectric–antiferroelectric morphotropic phase boundary controlled by flexoelectric interaction, Nat. Commun. **3**, 775 (2012).

[37] E. A. Eliseev, S. V. Kalinin, Y. Gu, M. D. Glinchuk, V. V. Khist, A. Y. Borisevich, V. Gopalan, L.-Q. Chen, and A. N. Morozovska, Universal emergence of spatially-modulated structures induced by flexo-antiferrodistortive coupling in multiferroics, Phys. Rev. B **88**, 224105 (2013).

[38] P. Henning and E. K. H Salje, Flexoelectricity, incommensurate phases and the Lifshitz point, J. Phys.: Condens. Matter **28**, 075902 (2016).

[39] J. Hong, First-principles theory of frozen-ion flexoelectricity, Phys. Rev. B **84**, 180101(R) (2011); I. Ponomareva, A. K. Tagantsev, and L. Bellaiche, Finite-temperature flexoelectricity in ferroelectric thin films from first principles, *ibid.* **85**, 104101 (2012).

[40] M. Stengel, Unified *ab initio* formulation of flexoelectricity and strain-gradient elasticity, Phys. Rev. B **93**, 245107 (2016).

[41] P. Zubko, G. Catalan, A. Buckley, P. R. L. Welche, and J. F. Scott, Strain-Gradient-Induced Polarization in $SrTiO_3$ Single Crystals, Phys. Rev. Lett. **99**, 167601 (2007).

[42] W. Ma and L. E. Cross, Flexoelectricity of barium titanate, Appl. Phys. Lett. **88**, 232902 (2006).

[43] W. Ma and L. E. Cross, Flexoelectric effect in ceramic lead zirconate titanate, Appl. Phys. Lett. **86**, 072905 (2005).

[44] *Flexoelectricity in Solids: From Theory to Applications*, edited byA. K. Tagantsev and P. V. Yudin (World Scientific, New Jersey, 2016), Chap. 6.

[45] P. V. Yudin and A. K. Tagantsev, Fundamentals of flexoelectricity in solids, Nanotechnology **24**, 432001 (2013).

[46] P. Zubko, G. Catalan, and A.K. Tagantsev, Flexoelectric effect in solids, Annu. Rev. Mater. Res. **43**, 387 (2013).

[47] M. Stengel, Flexoelectricity from density-functional perturbation theory, Phys. Rev. B **88**, 174106 (2013).

[48] A. Kvasov and A. K. Tagantsev, Dynamic flexoelectric effect in perovskites from first-principles calculations, Phys. Rev. B **92**, 054104 (2015).

[49] *Flexoelectricity in Solids: From Theory to Applications*, edited by A. K. Tagantsev and P. V. Yudin (World Scientific, New Jersey, 2016), Chap. 2.

[50] A. N. Morozovska, Y. M. Vysochanskii, O. V. Varenyk, M. V. Silibin, S. V. Kalinin, and E. A. Eliseev, Flexocoupling impact on the generalized susceptibility and soft phonon modes in the ordered phase of ferroics, Phys. Rev. B **92**, 094308 (2015).

[51] A. N. Morozovska, E. A. Eliseev, C. M. Scherbakov, and Y. M. Vysochanskii, The influence of elastic strain gradient on the upper limit of flexocoupling strength, spatially-modulated phases and soft phonon dispersion in ferroics, Phys. Rev. B **94**, 174112 (2016).

[52] R. Maranganti and P. Sharma, Atomistic determination of flexoelectric properties of crystalline dielectrics, Phys. Rev. B **80**, 054109 (2009).

[53] N. D. Sharma, C. M. Landis, and P. Sharma, Piezoelectric thin-film superlattices without using piezoelectric materials, J. Appl. Phys. **108**, 024304 (2010).

[54] E. A. Eliseev, A. N. Morozovska, M. D. Glinchuk, and S. V. Kalinin, Missed surface waves in non-piezoelectric solids, Phys. Rev. B **96**, 045411 (2017).

[55] B. A. Strukov and A. P. Levanyuk, *Ferroelectric Phenomena in Crystals* (Springer, Berlin, 1998).

[56] C. Kappler and M. B. Walker, Symmetry-based model for the modulated phases of betaine calcium chloride dihydrate, Phys. Rev. B **48**, 5902 (1993).

[57] J. Hlinka, M. Quilichini, R. Currat, and J. F. Legrand, Dynamical properties of the normal phase of betaine calcium chloride dihydrate. II. A semimicroscopic model, J. Phys.: Condens. Matter **8**, 8221 (1996).

[58] S. W. H. Eijt, R. Currat, J. E. Lorenzo, P. Saint-Gregoire, B. Hennion, and Yu M. Vysochanskii, Soft modes and phonon interactions in $Sn_2P_2S_6$ studied by neutron scattering, Eur. Phys. J. B **5**, 169 (1998).

[59] S. W. H. Eijt, R. Currat, J. E. Lorenzo, P. Saint-Gregoire, S. Katano, T. Janssen, B. Hennion, and Yu M. Vysochanskii, Soft modes and phonon interactions in $Sn_2P_2Se_6$ studied by means of neutron scattering, J. Phys.: Condens. Matter **10**, 4811 (1998).

[60] L. D. Landau and E. M. Lifshitz, *Theory of Elasticity. Theoretical Physics* (Butterworth-Heinemann, Oxford, U.K.,1998), Vol. 7.

[61] G. A. Smolenskii, V. A. Bokov, V. A. Isupov, N. N. Krainik, R. E. Pasynkov, and A. I. Sokolov, *Ferroelectrics and Related Materials* (Gordon and Breach, New York, 1984).

[62] Yu. M. Vysochanskii and V. Yu. Slivka, Lifshitz point on the state diagram of ferroelectric, Usp. Fiz. Nauk. **162**, 139 (1992).

[63] E. A. Eliseev, A. N. Morozovska, M. D. Glinchuk, and R. Blinc, Spontaneous flexoelectric/flexomagnetic effect in nanoferroics, Phys. Rev. B **79**, 165433 (2009).

[64] A. S. Yurkov, Elastic boundary conditions in the presence of the flexoelectric effect, JETP Letters **94**, 455 (2011).

[65] S. Mao and P. K. Purohit, Insights into flexoelectric solids from strain-gradient elasticity, J. Appl. Mech. **81**, 081004 (2014).

[66] R. Maranganti and P. Sharma, A novel atomistic approach to determination of strain-gradient elasticity constants: Tabulation and comparison for various metals, semiconductors, silica, polymers and the (ir) relevance for nanotechnologies, J. Mech. Phys. Solids **55**, 1823 (2007).

[67] See Supplemental Material at http://link.aps.org/supplemental/10.1103/PhysRevB.96.094111 for mathematical details.

[68] V. Yu. Korda, S. V. Berezovsky, A. S. Molev, L. P. Korda, and V. F. Klepikov, A possible generalization of the phenomenological theory of phase transitions in type II ferroelectrics with incommensurate phase, Phys. B **407**, 3388 (2012).

[69] V. Yu. Korda, A. S. Molev, L. P. Korda, and V. F. Klepikov, On importance of higher non-linear interactions in the theory of type II incommensurate systems, Physica B **425**, 31 (2013).

[70] K. Z. Rushchanskii, A. Molnar, R. Bilanych, R. Yevych, A. Kohutych, Yu. M. Vysochanskii, V. Samulionis, and J. Banys, Observation of nonequilibrium behavior near the Lifshitz point in ferroelectrics with incommensurate phase, Phys. Rev. B **93**, 014101 (2016).

[71] J. M. Perez-Mato, Symmetry analyses of the phase transition sequence in betaine calcium chloride dehydrate, Solid State Commun. **67**, 1145 (1988).

[72] E. A. Eliseev, A. N. Morozovska, M. D. Glinchuk, B. Y. Zaulychny, V.V. Skorokhod, and R. Blinc, Surface-induced piezomagnetic, piezoelectric, and linear magnetoelectric effects in nanosystems, Phys. Rev. B **82**, 085408 (2010).

[73] E. A. Eliseev, Complete symmetry analyses of the surface-induced piezomagnetic, piezoelectric and linear magnetoelectric effects, Ferroelectrics **417**, 100 (2011).

[74] K. Patel, S. Prosandeev, and L. Bellaiche, Dynamics of antipolar distortions, npj Comput. Mater. **3**, 34 (2017).